

Structural Reliability Assessment of a 4MW Offshore Wind Turbine





Structural Reliability Assessment of a 4MW Offshore Wind Turbine

Author(s)

J.M. Peeringa
G. Bedon

Disclaimer

Although the information contained in this document is derived from reliable sources and reasonable care has been taken in the compiling of this document, ECN cannot be held responsible by the user for any errors, inaccuracies and/or omissions contained therein, regardless of the cause, nor can ECN be held responsible for any damages that may result therefrom. Any use that is made of the information contained in this document and decisions made by the user on the basis of this information are for the account and risk of the user. In no event shall ECN, its managers, directors and/or employees have any liability for indirect, non-material or consequential damages, including loss of profit or revenue and loss of contracts or orders.

Acknowledgement

The Design for Reliable Power Performance (D4REL) project is partially sponsored by TKI Wind op Zee TKIWO2007. The ECN project number is 5.2611.

Leandro Orsi, Arno Brand, Marco Caboni and Koen Hermans are thanked for their contribution to work package 3.

Table of contents

Summary	5
1. Introduction	6
2. Metocean conditions	7
3. Structural reliability method	10
3.1 Methodology	10
3.2 Implementation of reliability method	12
4. Wind turbine model	14
5. Fatigue limit state	18
5.1 Introduction	18
5.2 Fatigue model	18
5.3 Structural reliability assessment	19
5.3.1 Fatigue limit state assessment for lumped, 4D scatter and a 20 years data set of sea states	20
5.3.2 Fatigue limit state assessment with fully integrated load analysis	22
5.3.3 Conclusions	24
6. Ultimate buckling limit state	25
6.1 Statistical extrapolation of wind turbine responses	25
6.1.1 Introduction	25
6.1.2 Number of time series and data selection	26
6.1.3 Short-term probability distributions	28
6.2 Selection of Ultimate Limit State function	28
6.3 Results	29
7. Assessment of partial safety factors	32
8. Uncertainty of soil properties	35
9. Conclusions	40
Bibliography	42

Summary

To make offshore wind energy cost effective there is a need to reduce the Cost of Energy (CoE). The aim of work package 3 of the D4REL project is to investigate where cost reductions in the support structure are possible while keeping a sound and safe design. Probabilistic design methods (structural reliability methods) are used to study whether there is any conservatism in the design of support structures.

For the probabilistic analysis, a modern 4MW offshore wind turbine is selected. In the probabilistic design approach, the limit state condition is adopted. The limit state function g is the difference between the resistance R and the load L . For a safe design the limit function should be larger than zero. In structural reliability the design point is determined where the limit state function is zero. Three limit state functions are considered:

1. A fatigue limit state;
2. An ultimate limit state on the yield stress;
3. An ultimate limit state on the global buckling stress.

A generic reliability analysis approach is taken by coupling the aeroelastic simulation tool TURBU with the open source reliability analysis tool FERUM. The First Order Reliability Method (FORM) is used since it calculates the influence of the stochastic variables with respect to the variance of the limit state function.

Based on the selected stochastic variables, the fatigue and ultimate buckling limit state show a smaller probability of failure than the target probability of 10^{-4} according to the standard. It is shown that the translation of this smaller probability of failure to a reduced partial safety factor is not straightforward.

In the ultimate limit state the uncertainty of the soil stiffness has a large influence. As requested by Van Oord, the uncertainty of the soil properties of the different soil layers is investigated. The contribution of the clay layer to the uncertainty of the limit state function is with 80-90% the largest.

1. Introduction

To make offshore wind energy cost effective there is a need to reduce the Cost of Energy (CoE). The aim of work package 3 of the D4REL project is to investigate where cost reductions in the support structure are possible, while keeping a sound and safe design. Probabilistic design methods (structural reliability methods) are used to study whether there is any conservatism in the design of support structures.

At this moment the design of support structures for offshore wind turbines is done through a collaboration between the wind turbine manufacture and a specialized support structure design company like Ramboll and Van Oord. The support structure consists of a foundation, a transition piece and a tower. The tower is designed by the wind turbine manufacturer, while the foundation and transition piece are designed by the engineering company. The structural design is subjected to partial safety factors as prescribed in the IEC61400-1 standard or the DNV-OS-J101 standard. Partial safety factors are applied to compensate for uncertainties in the design process. Improved knowledge may help to reduce these factors and hence contribute to reduction in Cost of Energy (CoE) without compromising the reliability of the design.

As an alternative to apply partial safety factors, probabilistic design methods can be considered. In the past, for instance the Prodeto project, probabilistic design methods were already used by ECN for wind turbines. The focus in this work package will lay on the support structure while taking the complete offshore wind turbine system into account.

The goal of this report is to present the results of the probabilistic analysis for the generic ECN 4MW wind turbine. First the metocean data and the wind turbine used in the analysis are discussed, followed by a description of the generic probabilistic analysis approach applied. The probabilistic analysis is performed for the fatigue limit case and the ultimate buckling limit state as reported in chapter five and six respectively. The results of the fatigue and ultimate limit state analysis are applied in chapter seven to determine the partial safety factors of the stochastic variables.

In the ultimate limit state, the uncertainty of the soil stiffness has a large influence. In chapter eight the uncertainty of the soil properties of the different soil layers is investigated.

2. Metocean conditions

For the probabilistic analysis the wind and wave loads on the offshore wind turbine are calculated for site-specific environmental conditions. The selected site is located North of the Dutch Wadden Isles in 30m water depth. For the selected location two sources were used for the environmental data.

1. DHI-WASY metocean report[15];
2. Twenty years of hindcast data as provided by Argos.

The number of sea states taken into account during the load calculation largely determines the computational effort needed for the probabilistic analysis. Three metocean data sets with a different number of sea states are considered.

1. A complete set of 20-year three-hours metocean hindcast data
2. 4D-histogram of binned mean wind speed u , significant wave height H_s , wave peak period T_p and wind wave misalignment θ ;
3. A lumped data set of twelve three-hour sea states.

The lumped sea states are based on two-dimensional scatter diagrams as provided in the appendices of the metocean report [15]. The lumped sea states are based on the bins in the scatter diagram with the highest occurrences. Figure 2-1 shows the significant wave height H_s and the mean wind speed at hub height u . Figure 2-2 shows the significant wave height H_s versus the wave peak period T_p .

Table C-49 (Doc 144268-DHI AppC_Scatter 20120523 - Copy.pdf)

Hm0 (m)	Wind speed at hub height (m/s)																					
	0-2	2-4	4-6	6-8	8-10	10-12	12-14	14-16	16-18	18-20	20-22	22-24	24-26	26-28	28-30	30-32	32-34	34-36	36-38	All		
9.00-9.25	C	0	0	0	0	0	C	0	0	0	0	0	C	2	0	0	0	0	0	C	2	
8.75-9.00	C	0	0	0	0	0	C	0	0	0	0	0	C	2	2	0	0	0	0	0	C	4
8.50-8.75	C	0	0	0	0	0	C	0	0	0	0	0	1	C	0	0	0	0	0	0	C	1
8.25-8.50	C	0	0	0	0	0	C	0	0	0	0	0	0	C	4	5	1	0	0	0	C	10
8.00-8.25	C	0	0	0	0	0	C	0	0	0	0	0	0	C	7	2	0	0	0	0	C	9
7.75-8.00	C	0	0	0	0	0	C	0	0	0	0	0	1	2	12	9	1	0	0	0	C	25
7.50-7.75	C	0	0	0	0	0	C	0	0	0	0	1	2	15	22	6	1	1	0	0	C	48
7.25-7.50	C	0	0	0	0	0	C	0	0	0	0	0	1	21	28	13	2	1	2	1	C	70
7.00-7.25	C	0	0	0	0	0	C	0	0	0	0	2	13	35	24	5	1	0	1	1	C	81
6.75-7.00	C	0	0	0	0	0	C	0	0	0	0	4	20	41	33	5	1	0	0	0	C	106
6.50-6.75	C	0	0	0	0	0	C	0	0	0	0	6	40	59	26	5	0	0	1	1	C	137
6.25-6.50	C	0	0	0	0	0	C	0	0	0	0	18	74	77	15	2	1	1	0	0	C	190
6.00-6.25	C	0	0	0	0	0	C	0	0	1	47	129	59	11	5	0	0	0	0	0	C	252
5.75-6.00	C	0	0	0	0	0	C	0	0	9	94	149	51	9	2	1	0	0	0	0	C	315
5.50-5.75	C	0	0	0	0	0	C	0	1	47	172	141	40	8	0	0	0	0	0	0	C	408
5.25-5.50	C	0	0	0	0	0	C	0	4	87	247	145	19	3	0	1	0	0	0	0	C	504
5.00-5.25	C	0	0	0	0	0	C	1	19	219	304	154	24	1	0	0	0	0	0	0	C	718
4.75-5.00	C	0	0	0	0	0	C	3	68	353	407	128	9	1	0	0	0	0	0	0	C	968
4.50-4.75	C	0	0	0	0	0	1	11	199	543	386	107	6	0	0	0	0	0	0	0	C	1253
4.25-4.50	C	0	0	0	0	0	1	31	464	721	427	72	7	0	0	0	0	0	0	0	C	1723
4.00-4.25	C	0	0	0	0	2	6	142	753	848	381	38	1	0	0	0	0	0	0	0	C	2172
3.75-4.00	C	0	0	0	0	1	38	417	1091	1034	272	19	1	0	0	0	0	0	0	0	C	2873
3.50-3.75	C	0	0	0	3	6	129	900	1458	888	163	6	1	0	0	0	0	0	0	0	C	3554
3.25-3.50	C	0	0	0	3	41	353	1382	1607	688	80	2	C	0	0	0	0	0	0	0	C	4136
3.00-3.25	C	0	0	2	16	136	879	2031	1818	509	29	1	C	0	0	0	0	0	0	0	C	5421
2.75-3.00	C	0	0	6	54	363	1663	2581	1759	249	10	0	C	0	0	0	0	0	0	0	C	6885
2.50-2.75	C	1	3	32	200	1004	2973	3054	1344	84	1	1	C	0	0	0	0	0	0	0	C	8997
2.25-2.50	C	4	23	110	530	2166	4061	3252	896	26	0	0	C	0	0	0	0	0	0	0	C	10868
2.00-2.25	1	21	67	345	1300	3762	5027	2533	191	4	2	1	C	0	0	0	0	0	0	0	C	13254
1.75-2.00	23	97	277	882	2726	5864	5294	1297	41	3	0	0	C	0	0	0	0	0	0	0	C	16504
1.50-1.75	72	294	874	2183	5445	7635	4272	329	8	0	0	0	C	0	0	0	0	0	0	0	C	21112
1.25-1.50	230	714	2084	4549	8272	8372	1690	51	2	0	0	0	C	0	0	0	0	0	0	0	C	25964
1.00-1.25	497	1944	4246	8220	11847	5263	246	12	0	0	0	0	C	0	0	0	0	0	0	0	C	32275
0.75-1.00	1091	3622	7747	12724	10392	967	26	2	0	0	0	0	C	0	0	0	0	0	0	0	C	38571
0.50-0.75	1734	5701	12047	12524	2431	53	2	1	0	0	0	0	C	0	0	0	0	0	0	0	C	34493
0.25-0.50	2462	7170	6964	1535	76	2	C	0	0	0	0	0	C	0	0	0	0	0	0	0	C	18208
0.00-0.25	928	2389	1149	132	9	1	C	1	0	0	0	0	C	0	0	0	0	0	0	0	C	4588
All	7038	21937	35481	43244	43304	35640	26662	18031	11523	6293	3063	1243	471	208	61	10	3	4	1	254208		

Figure 2-1 Scatter diagram of mean wind speed at hub height U and the significant wave height Hs.

Table C-1 (Doc 144268-DHI AppC_Scatter 20120523 - Copy.pdf)

Hm0 (m)	Tp (s)																	all				
	0-1	1-2	2-3	3-4	4-5	5-6	6-7	7-8	8-9	9-10	10-11	11-12	12-13	13-14	14-15	15-16	16-17					
9.00-9.25	0	0	0	0	0	C	0	0	0	0	0	C	0	0	2	0	0	0	0	C	2	
8.75-9.00	0	0	0	0	0	C	0	0	0	0	0	C	1	1	2	0	0	0	0	0	C	4
8.50-8.75	0	0	0	0	0	C	0	0	0	0	0	C	0	0	1	0	0	0	0	0	C	1
8.25-8.50	0	0	0	0	0	C	0	0	0	0	0	6	3	1	0	0	0	0	0	0	C	10
8.00-8.25	0	0	0	0	0	C	0	0	0	0	0	7	1	1	0	0	0	0	0	0	C	9
7.75-8.00	0	0	0	0	0	C	0	0	0	0	1	21	2	0	1	0	0	0	0	0	C	25
7.50-7.75	0	0	0	0	0	C	0	0	0	0	4	31	7	5	1	0	0	0	0	0	C	48
7.25-7.50	0	0	0	0	0	C	0	0	0	0	16	41	10	2	0	0	0	0	0	0	C	70
7.00-7.25	0	0	0	0	0	C	0	0	0	0	31	31	11	7	1	0	0	0	0	0	C	81
6.75-7.00	0	0	0	0	0	C	0	0	0	1	47	48	3	6	1	0	0	0	0	0	C	106
6.50-6.75	0	0	0	0	0	C	0	0	0	17	53	60	1	6	0	0	0	0	0	0	C	137
6.25-6.50	0	0	0	0	0	C	0	0	3	42	71	65	1	8	0	0	0	0	0	0	C	190
6.00-6.25	0	0	0	0	0	C	0	0	5	47	127	59	2	12	0	0	0	0	0	0	C	252
5.75-6.00	0	0	0	0	0	C	0	0	8	75	174	51	1	6	0	0	0	0	0	0	C	315
5.50-5.75	0	0	0	0	0	C	0	0	16	115	210	67	1	5	0	0	0	0	0	0	C	408
5.25-5.50	0	0	0	0	0	C	0	0	22	196	248	34	0	6	0	0	0	0	0	0	C	504
5.00-5.25	0	0	0	0	0	C	0	0	68	350	272	25	0	3	0	0	0	0	0	0	C	718
4.75-5.00	0	0	0	0	0	C	0	3	165	511	276	10	1	3	0	0	0	0	0	0	C	968
4.50-4.75	0	0	0	0	0	C	0	28	331	659	234	4	2	5	0	0	0	0	0	0	C	1253
4.25-4.50	0	0	0	0	0	C	0	52	681	781	193	6	1	9	0	0	0	0	0	0	C	1723
4.00-4.25	0	0	0	0	0	C	0	194	1000	843	125	4	3	3	0	0	0	0	0	0	C	2172
3.75-4.00	0	0	0	0	0	C	3	426	1436	918	79	8	1	2	0	0	0	0	0	0	C	2873
3.50-3.75	0	0	0	0	0	C	21	866	1827	759	60	11	4	6	0	0	0	0	0	0	C	3554
3.25-3.50	0	0	0	0	0	C	83	1549	1880	560	40	11	5	8	0	0	0	0	0	0	C	4136
3.00-3.25	0	0	0	0	0	C	323	2632	1974	446	30	11	0	4	0	0	0	0	0	0	C	5421
2.75-3.00	0	0	0	0	0	10	919	3521	1836	344	28	15	5	7	0	0	0	0	0	0	C	6885
2.50-2.75	0	0	0	0	0	84	2011	4365	1823	341	51	8	9	6	0	0	0	0	0	0	C	8997
2.25-2.50	0	0	0	0	1	396	3794	4512	1745	319	72	11	15	1	0	0	0	0	0	0	C	10868
2.00-2.25	0	0	0	0	11	1331	5578	4281	1527	386	100	29	6	3	0	0	0	0	0	0	C	13254
1.75-2.00	0	0	0	1	115	3510	6564	4231	1475	394	152	51	12	2	0	0	0	0	0	0	C	16504
1.50-1.75	0	0	0	2	923	6421	6884	4348	1643	604	219	51	12	0	0	0	0	0	0	0	C	21112
1.25-1.50	0	0	0	22	3286	8283	6959	4526	2030	643	190	21	0	0	0	0	0	0	0	0	C	25964
1.00-1.25	0	0	0	376	8084	8721	7395	5274	1958	413	41	7	0	0	0	0	0	0	0	0	C	32275
0.75-1.00	0	0	10	3054	11274	10131	6840	4074	1059	119	5	1	0	0	0	0	0	0	0	0	C	38571
0.50-0.75	0	0	319	10258	11167	6988	4064	1519	163	7	7	1</										

The applied definition of the peak shape parameter is according to DNV-RP-C205 [8].

$$\gamma = 5 \text{ for } \frac{T_p}{\text{sqrt}(H_s)} \leq 3.6$$

$$\gamma = \exp(5.75 - 1.15 * \left(\frac{T_p}{\text{sqrt}(H_s)}\right)) \text{ for } 3.6 < \frac{T_p}{\text{sqrt}(H_s)} < 5$$

$$\gamma = 1 \text{ for } 5 \leq \frac{T_p}{\text{sqrt}(H_s)}$$

Table 2-1 Twelve lumped sea states.

Case	Wind velocity	Significant wave height	Spectra Peak Period	peak shape parameter (γ)
	[m/s]	[m]	[s]	[-]
1	3	0.375	4.5	1.00
2	5	0.625	4.5	1.00
3	7	0.875	4.5	1.24
4	9	1.125	5.5	1.00
5	11	1.375	5.5	1.43
6	13	1.875	6.5	1.34
7	15	2.375	7.5	1.17
8	17	3.125	7.5	2.39
9	19	3.875	8.5	2.19
10	21	4.375	9.5	1.69
11	23	5.125	9.5	2.52
12	25	6.375	10.5	2.63

The probability of occurrence of a lumped sea state is determined using a Weibull distribution of the mean wind speed with shape parameter k of 2.15 and scale parameter c of 10.57.

The 4D scatter histogram is based on the twenty year three-hour metocean sea states binned over the mean wind speed at hub height, wind-wave misalignment, the significant wave height and wave peak period. Only the wind bins between cut-in 4m/s and cut-out wind speed 25m/s are considered with a bin width of 2m/s. The significant wave height is binned with a bin width of 0.50m between 0.25m and 9.25m. The wave peak period is binned with a bin width of 0.5s between 1.75s and 23.75s. Finally the wind-wave misalignment is binned with a bin width of 30deg between 0deg and 360deg. For every bin, the number of occurrences in the twenty year data set is counted. The probability of occurrence of the bin can therefore be determined and applied in the probabilistic analysis.

3. Structural reliability method

3.1 Methodology

In the probabilistic design approach the limit state condition is considered. The limit state function g is the difference between the material resistance R and the load strength S .

$$g = R - S$$

For a safe design the limit function should be larger than zero. In structural reliability, the design point is determined where the limit state function is zero. The design point is the shortest distance to the mean of the stochastic material resistance and load strength variables. Three limit state functions are considered:

1. A fatigue limit state;
2. An ultimate limit state on the yield stress;
3. An ultimate limit state on the global buckling stress.

In probabilistic analysis the variables R and S are described by a probability density function. The shaded area in Figure 3-1 corresponds with the probability of failure, where load S is larger than resistance R .

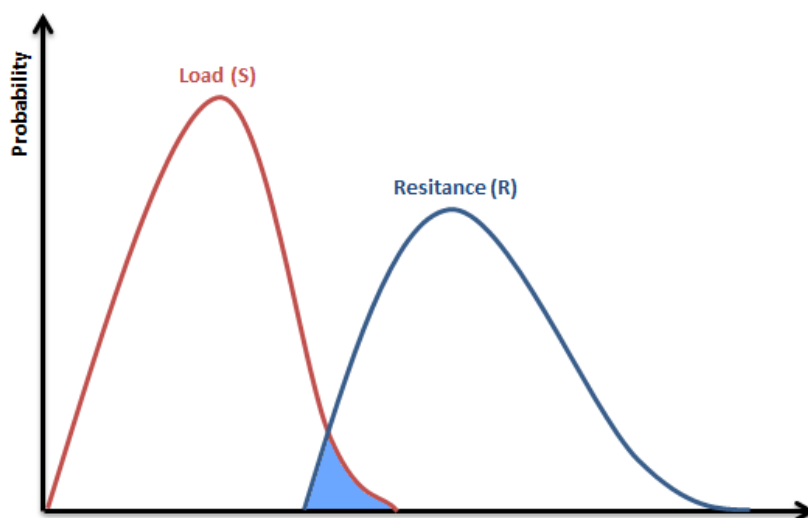


Figure 3-1 Probability load Strength S and material resistance R . The blue area is the probability of failure [2].

In the frame work report [2] for reliability assessment it was decided to apply level III methods, where the stochastic variables are modelled by their distribution functions. Several methods are available:

- Simulation techniques, where samples of the stochastic variables are generated and the relative number of samples is used to estimate the probability of failure. The simulation techniques like Monte Carlo can be used as validation for more complex techniques like FORM and SORM (see below).
- First Order Reliability Method (FORM) techniques, where limit state function is linearized and the reliability is estimated using level III methods.
- Second Order Reliability Method (SORM) techniques, where a quadratic approximation to limit state function is determined and probability of failure for the quadratic failure surface is estimated.

The FORM techniques, Figure 3-2, are a suitable option for reliability assessment of monopile structures. The advantage of FORM is the information on the importance of the selected stochastic variables to the total variance of the limit state function. Therefore, a FORM based reliability tool will be used in this report. Tools based on the FORM method result in a reliability index β , which is a measure of the reliability of a component. The reliability index is defined in the equation below, where $\Phi()$ is the standardised normal distribution function and $P_F(t)$ is the cumulative probability of failure in time interval t .

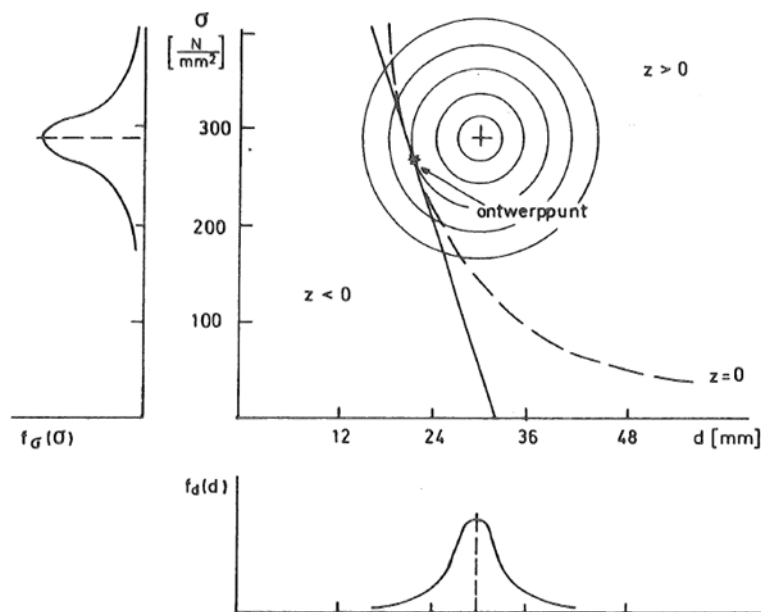


Figure 3-2 First Order Reliability Method (FORM)[31] .

$$\beta(t) = -\Phi^{-1}(P_F(t))$$

Figure 3-3 shows a definition in case the limit state g is normal distributed.

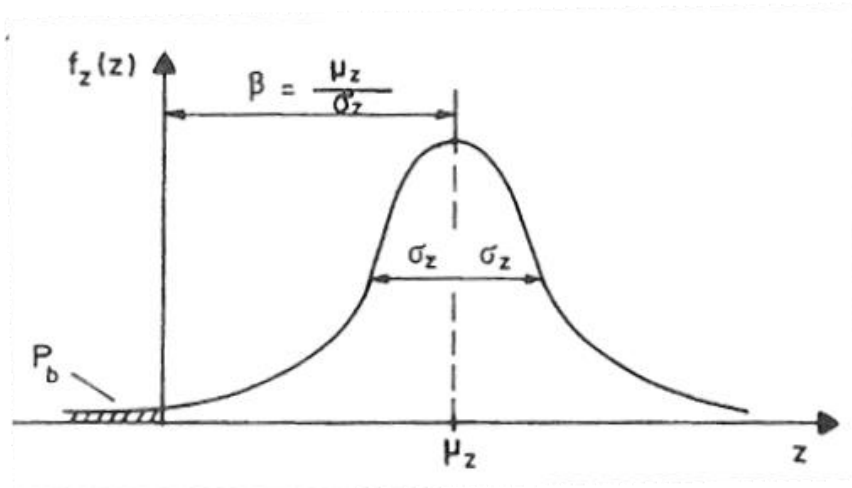


Figure 3-4 Probability of limit state Z [31].

3.2 Implementation of reliability method

A fully integrated load analysis is included in the structural reliability method of a monopile supported offshore wind turbine. To do so, TURBU is coupled with the reliability analysis tool FERUM [4]. FERUM considers a set of stochastic variables and iteratively varies them in order to find the zero of a limit state function, i.e. the design point. In the search for the design point, stochastic input variables can be included in the analysis, where the load set is recalculated in case the input is changed. The limit state function value represents the failure state for the wind turbine. Two criteria are adopted to assess convergence of the iterative algorithm:

- Relative residual: convergence is reached when

$$\frac{g}{g_0} < e_1$$

With g and g_0 being the limit state function values at the current and initial step respectively and e_1 the considered tolerance level (in this analysis 10^{-2})

- Step in gradient direction: convergence is reached when

$$x_i - \alpha^T \cdot x_i \cdot \alpha < e_2$$

With x_i being the current set of stochastic values, e_2 the considered tolerance level (in this analysis 10^{-2}) and α the unit vector in the gradient direction:

$$\alpha = \frac{\nabla g}{|\nabla g|}$$

A flowchart representing the steps performed in the coupled tool is shown in Figure 3-5. The loads as provided by TURBU are updated only if the load input variables vary from the previous calculated cases.

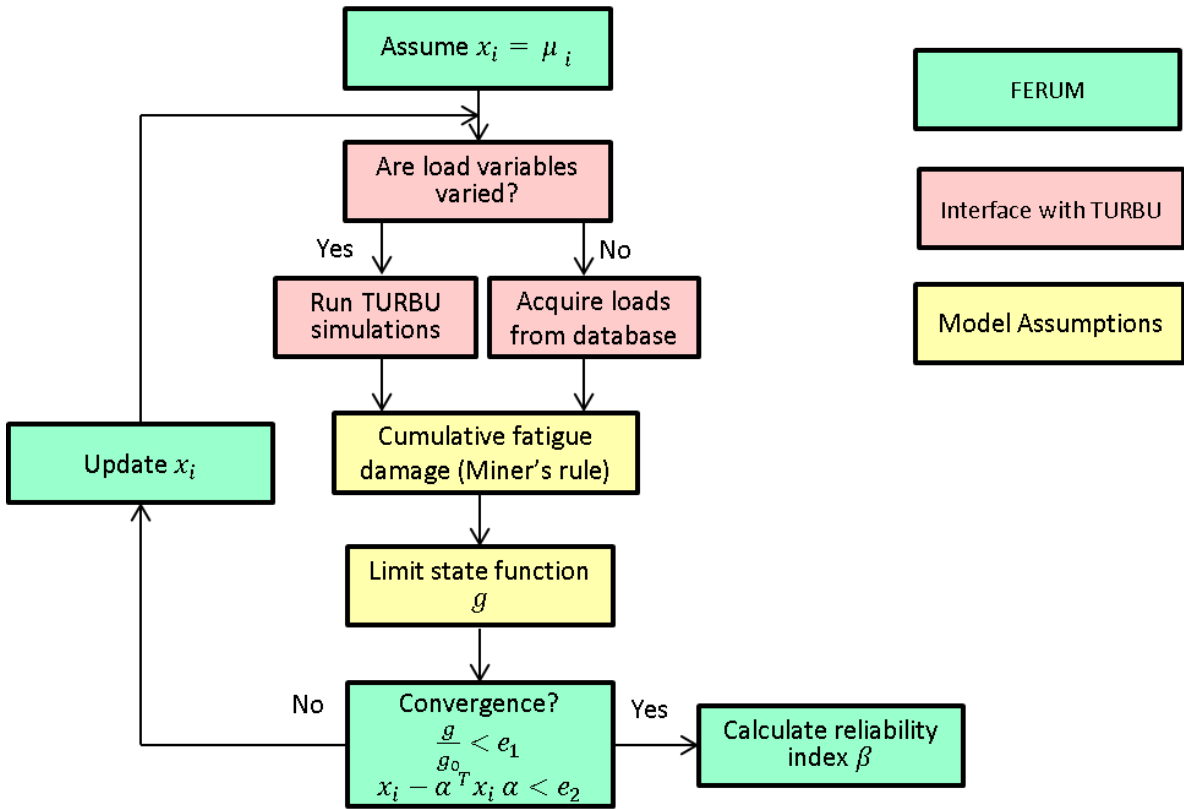


Figure 3-5 Flowchart for the coupled reliability analysis tool.

4. Wind turbine model

The use of nonlinear aeroelastic codes like PHATAS [17] for design load calculations is necessary. The drawback of these nonlinear tools is the required computational time, which is longer than real time. In the D4REL project, the number of simulated load cases during a reliability analysis is larger than the number of load cases required during standard design. Each time stochastic input variables change, a recalculation of the load set is needed in the search for the design point. A good alternative is the linear aeroelastic ECN code TURBU [29], which requires only a limited amount of time to compute a number of one hour time series. In the We-at-Sea project Turbu@Sea [23], ECN showed already that the correspondence between PHATAS and TURBU is good. TURBU models the wind turbine with sufficient accuracy.

In the D4REL project, the same generic ECN 4MW wind turbine as modelled in the WiFi-JIP project is used [22]. A TURBU model is created, considering the ART 5MW model [3] as a base. To achieve a model that was close to the required specifications, changes were made to the tower, the blades and the controller. The main characteristics are reported in Table 4-1

Table 4-1 Main characteristics of the reference 4MW wind turbine.

Rotor diameter [m]	130.0
Hub height (above mean sea level) [m]	92.4
Tower top (above mudline) [m]	117.0
Pile diameter (at mudline) [m]	7.0
Average water depth [m]	30.0

The first two bending modes of the support structure are shown in Figure 4-1.

The implementation of TURBU is based on a modular linear model, with control loops included: for the model details, the reader is addressed to references [29, 23]. Savenije and Peeringa [23] already presented that the comparison between the bending moment the power spectral densities estimated by the validated non-linear time domain code PHATAS [25] and TURBU shows

good overall agreement across the whole operating range. Also for the TURBU and PHATAS models of the generic ECN 4MW wind turbine, the power spectral density of the for-aft and side-way tower bending moments are compared for a wind speed below rated 8m/s and above rated 15m/s. The for-aft bending moment below rated shows good comparison up to about 0.5Hz, Figure 4-2. Above rated, the correspondence between PHATAS and TURBU up to 1Hz is good, Figure 4-3. For the side-way bending moment, the comparison is good for both below and above rated up to the second tower bending mode (1.25Hz). See Figure 4-4 and Figure 4-5. It is concluded that the TURBU model is accurate enough to apply in the load calculations.

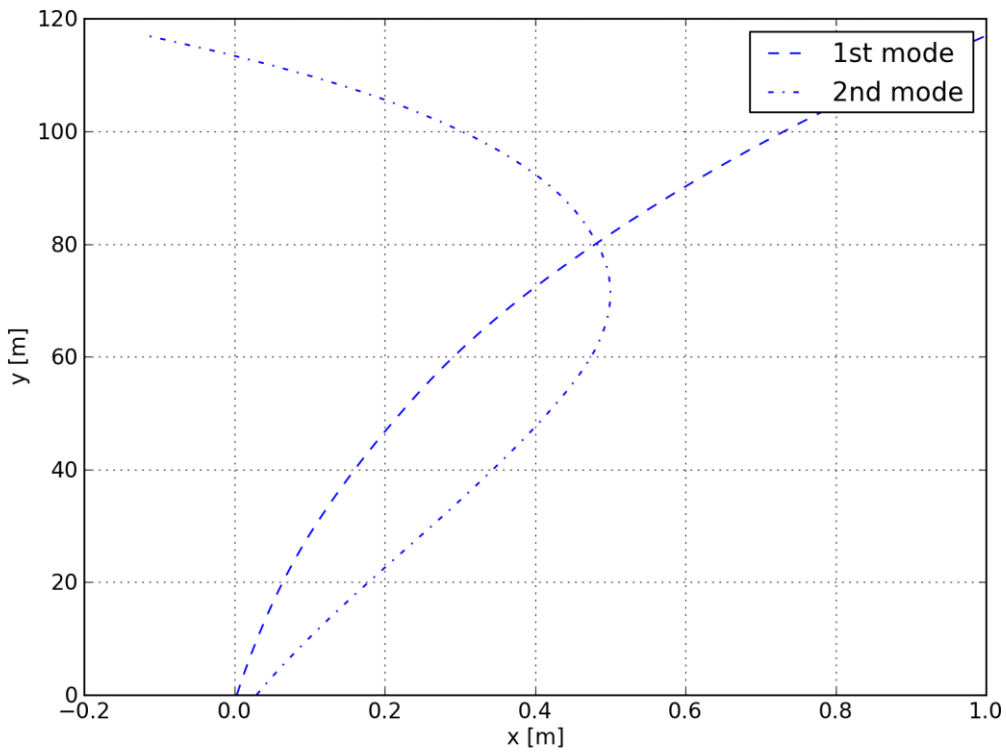


Figure 4-1 First two bending modes of the support structure.

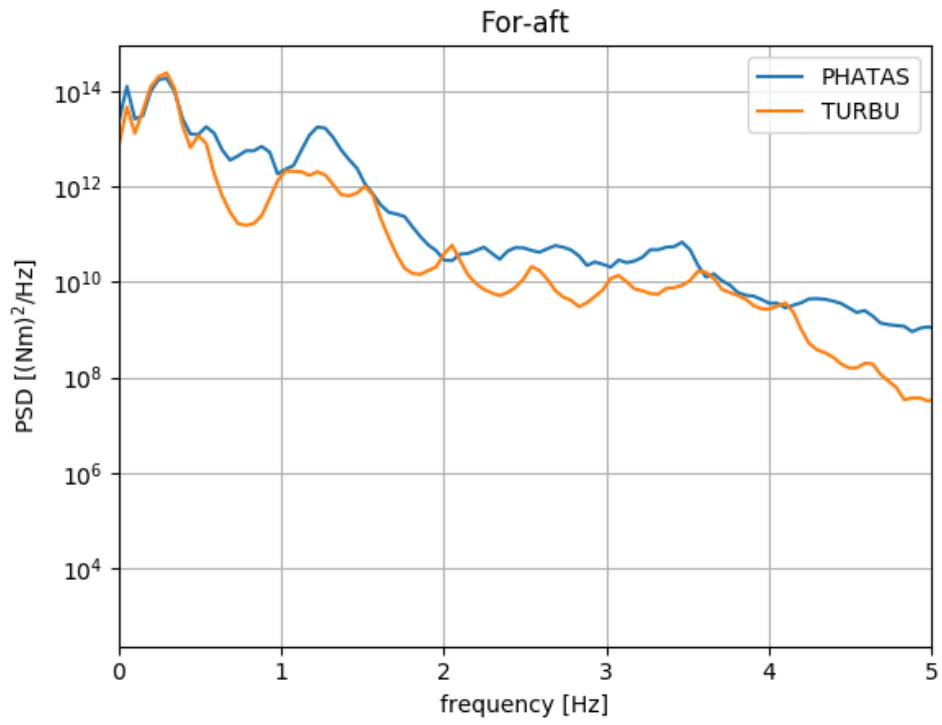


Figure 4-2 Power spectral density of for-aft tower bending moment at 8m/s wind speed.

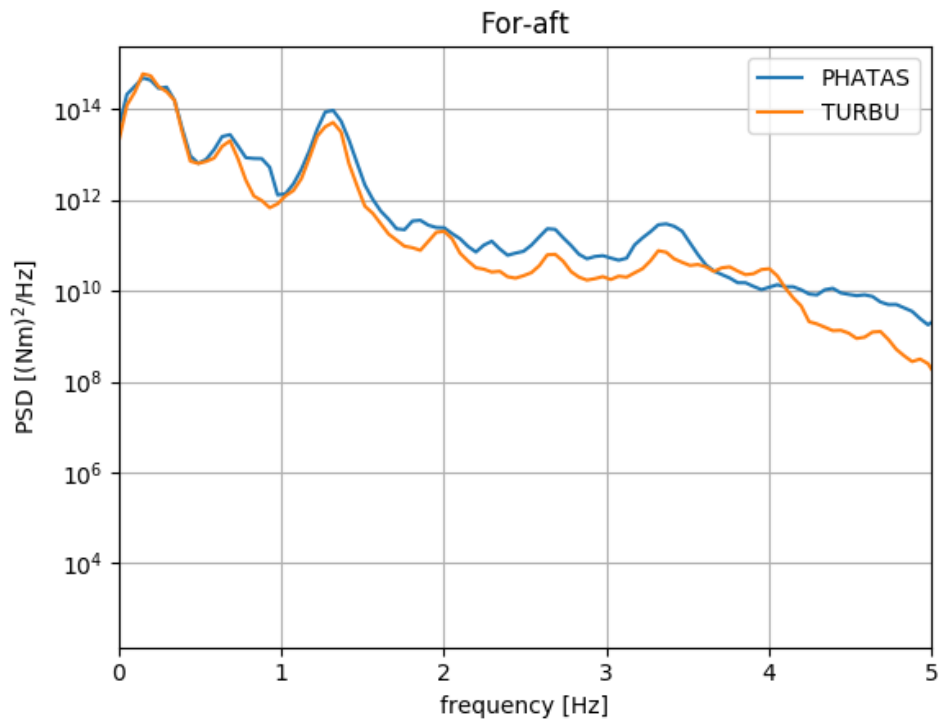


Figure 4-3 Power spectral density of for-aft tower bending moment at 15m/s wind speed

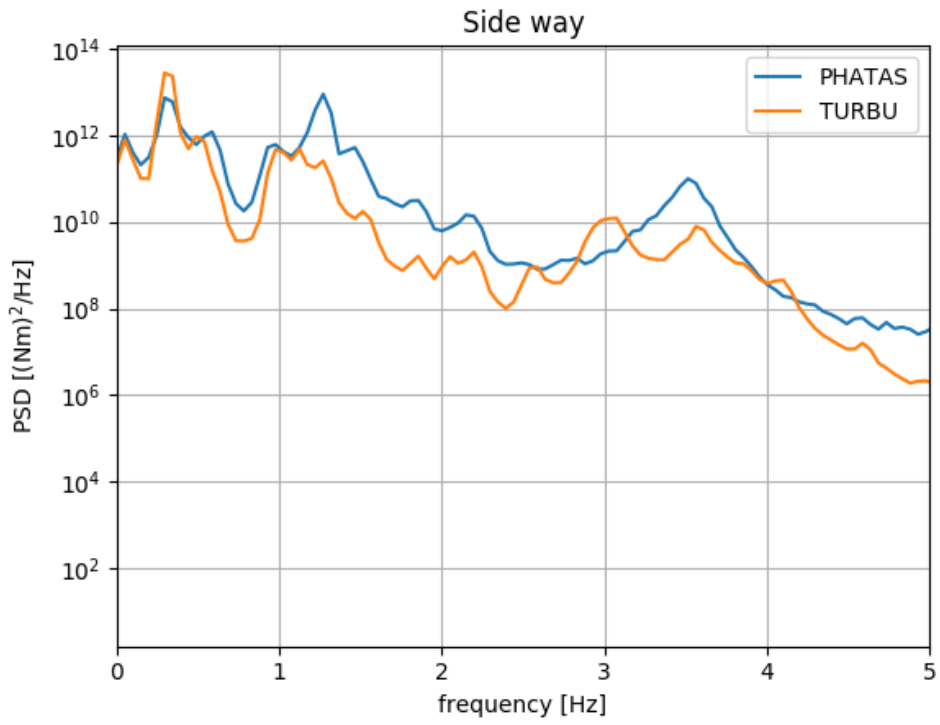


Figure 4-4 Power spectral density of side way tower bending moment at 8m/s wind speed

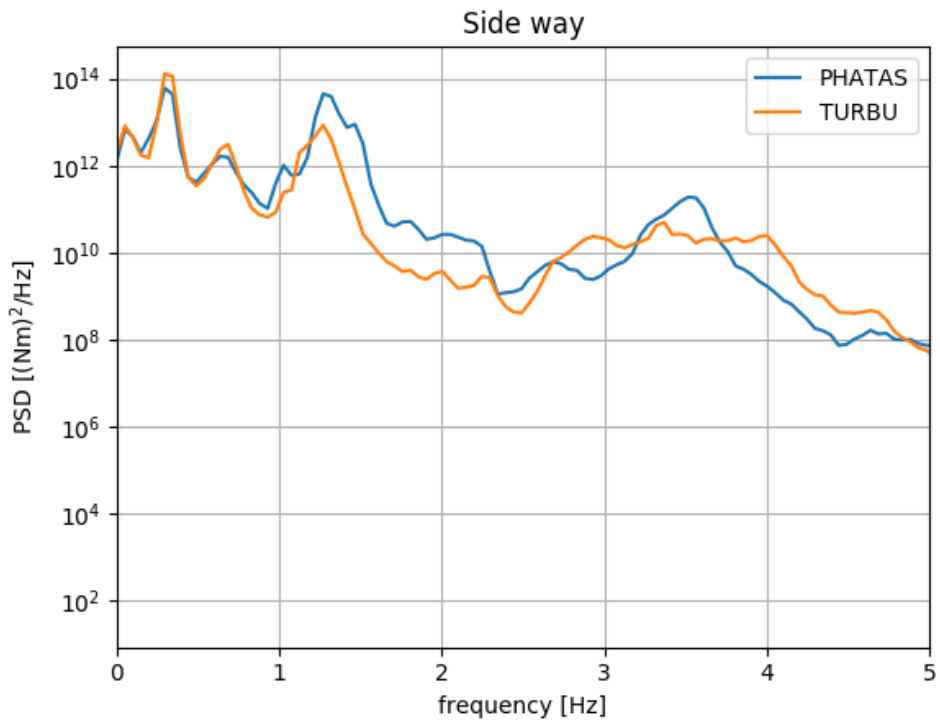


Figure 4-5 Power spectral density of side way tower bending moment at 15m/s wind speed

5. Fatigue limit state

5.1 Introduction

The reliability analysis is performed with the aim to obtain a reliability factor β and the inherent failure probability for a structure. These values should be compared with the values provided by the normative DNV OS-J101 [11], which prescribes a failure probability of 10^{-4} and 10^{-5} for unmanned and manned offshore structures respectively.

5.2 Fatigue model

The total fatigue damage D is then calculated by using the Palmgren-Miner rule as follows:

$$D = \sum_{i=1}^N \frac{n_i}{N_i}$$

where i refers to the bending moment bin and n_i are the stress cycles experienced during 20 year lifetime.

The stress range $\Delta\sigma_i$ is calculated using the Navier formula:

$$\Delta\sigma_i = \frac{\Delta M D_{out}}{I} \frac{1}{2}$$

where ΔM is the bending moment range and I the area inertia, estimated as

$$I = \pi \frac{D_{out}^4 - D_{in}^4}{64}$$

where D_{out} and D_{in} are respectively the external and internal diameter of the tower bottom.

For each stress range, $\Delta\sigma_i$, the fatigue life was calculated by means of a two-slope S-N curve. N_i is the number of stress cycles to failure at $\Delta\sigma_i$. The two-slope S-N curve considered was taken from the Offshore Standards DNV-OS-J101 [11] for a weld in a tubular joint, in seawater with cathodic protection (Curve T).

The two-slope S-N curve is represented by the following equation:

$$N_i = 10^{\log_{10} a} \left[\Delta \sigma_i \left(\frac{t}{t_{ref}} \right)^k \right]^{-m}$$

where

- $\log_{10} a$ is 11.764 for N_i lower than 10^6 , and 15.606 for N_i greater than 10^6 .
- t is the tower wall thickness at the considered tower height in m.
- t_{ref} is the reference thickness equal to 0.032 m.
- m is the negative slope of the S-N curve on logN-logS plot. It was set equal to 3 for N_i lower than 10^6 , and 5 for N_i greater than 10^6 .

5.3 Structural reliability assessment

The fatigue limit state g is defined. This should be zero when the turbine fails, so when fatigue damage D equals to 1. The adopted limit state function is:

$$g = \Delta - D$$

where Δ is the model uncertainty, assumed with mean of 1 and standard deviation of 0.30.

The reliability analysis is conducted by considering both the First Order Reliability Method (FORM) and the Second Order Reliability Method (SORM). The reliability index β and the failure probability p_F for a given set of stochastic variables are provided. The target failure probability for this type of applications is 10^{-4} , considering a reference period of 20 years as suggested by DNV-GL is. This approximately corresponds to a reliability index β of 3.8.

The cumulative damage D is calculated considering Miner's rule and the rain flow count of the for-aft bending moment at the mudline. The mudline is considered as reference structural location because preliminary analyses on the baseline design indicated the highest standard deviation of the stress in that section, as showed in Figure 5-1. Maximum fatigue loads are therefore assumed to occur in this section, which can be considered as design-driving. A complete reliability analysis for every tower section is not practical due to the excessive computational time.

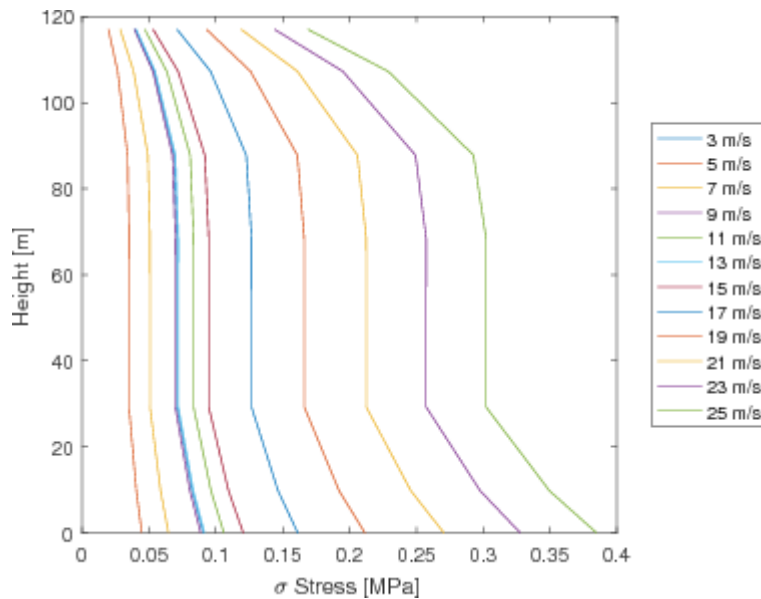


Figure 5-1 Standard deviation of the bending stress with respect to the tower section for different wind speeds.

The choice of stochastic and deterministic variables is of great importance to the final result of the sensitivity analysis. A selection based on literature studies [26, 27, 30] and international standards [9, 14] is conducted in the present analysis to perform the most reliable estimation of the reliability index. The values of the stochastic variables are reported in Table 5-1 and Table 5-3. Different reliability campaigns were performed considering multiple sets of variables. An uncertainty on the linear TURBU model is not explicitly considered as it is included in the uncertainties in the input parameters and in the Miner's rule. Moreover, different simulations are conducted considering the same input parameters but different stochastic seeds. Therefore the output provided by the model varies. This approach has the advantage of avoiding the estimation of a model uncertainty and is adopted also by authors in literature [34, 35].

In this report the results of two different structural reliability assessments on fatigue will be discussed. The first assessment has three different sized metocean data sets. For each data set the fatigue load cases are calculated in advance. The structural reliability assessment is on the response only.

The second assessment is a fully integrated one. Now also the selected stochastic input parameters are part of the structural reliability assessment. This means that each time the value of the input parameters change during the assessment the fatigue load cases should be recalculated for the new input.

5.3.1 Fatigue limit state assessment for lumped, 4D scatter and a 20 years data set of sea states

To investigate the sensitivity of the load analysis on the number of sea-states considered in the structural reliability analysis, three different sized data sets with sea states are considered.

1. A complete set of 20-year three-hours metocean hindcast data
2. 4D-histogram of binned mean wind speed u , significant wave height H_s , wave peak period T_p and wind wave misalignment θ ;
3. A lumped data set of 12 three-hour sea states.

For all data sets three yaw misalignments are considered -8deg, 0deg and 8deg for each sea state. For the lumped case two one hour simulations are performed using two seeds for every yaw

misalignment. For the scatter and lifetime data set one one-hour simulation is done for each yaw misalignment.

The fatigue life is calculated for twenty years. In case of the 4D-histogram the sea state is weighted for the occurrence in twenty years based on the histogram. In case of the lumped data set the sea states are weighted by the occurrence of the wind speeds. The wind speeds are distributed considering a Weibull distribution with shape parameter k of 2.15 and scale parameter c of 10.57 representing the site-specific wind conditions.

Because of the computational time involved in simulating the loads of a 20-year dataset, the fatigue load cases are calculated in advance. The stochastic variables selected are related to the damage calculation, like Δ for Miner's rule and $\log(C1)$ and $\log(C2)$ for the SN-curve. See Table 5-1.

Table 5-1 Stochastic variables adopted in the reliability analysis for the different metocean data sets.

Variable	Unit	distribution	M	σ	Reference
Log(C1) SN-curve	Log(Pa ³)	Normal	12.164	0.2	[18]
Log(C2)SN-curve	Log(Pa ⁵)	Normal	16.106	0.25	[18]
Δ (Miner's rule)	-	Lognormal	1	0.3	[9]

The reliability index β and the probability for the different metocean data sets are presented in Table 5-2. The target reliability of DNV-GL is met by all data sets. However looking at the probability of failure there is orders of difference. Based on the analysis the lumped data set is the most conservative one.

Table 5-2 Results of reliability assessment with different metocean data sets

Metocean data	β	Probability
Lumped	6.1	6.55E-10
4D histogram	8.3	5.47E-17
20-year hindcast	7.0	1.35E-12

Different β values are observed depending on the metocean data set. Meaning that content of the metocean data set matters. The lumped one shows the most conservative result.

5.3.2 Fatigue limit state assessment with fully integrated load analysis

Due to the computational time involved the lumped metocean data set is selected for the fully integrated load analysis.

The stochastic variables considered in the analysis are given in Table 5-3.

Table 5-3 Stochastic variables adopted in the reliability analysis with fully integrated load analysis.

Variable	Unit	Distribution	μ	σ	CoV	Reference
Log(C1) SN-curve	Log(Pa ³)	Normal	12.164	0.2	-	[18]
Log(C2)SN-curve	Log(Pa ⁵)	Normal	16.106	0.25	-	[18]
Δ (Miner's rule)	-	Lognormal	1	0.3	-	[9]
E Young's modulus	Pa	Lognormal	210E9	-	0.02	[26]
C_D	-	Normal	0.7	0.1	-	[30]
C_M	-	Normal	2.0	0.1	-	[30]
Soil stiffness	Nm/rad	Lognormal	6.603E10	-	0.2	[14]

The results of the fully integrated fatigue assessment are reported in Table 5-4 along with the number of limit state function (LSF) calls. The β values are sensibly higher than the value prescribed by DNV-GL.

Table 5-4 Results for the reliability analysis with fully integrated load analysis.

Analysis	β [-]	p_F [-]	LSF calls [-]
FORM	6.35	1.08E-10	219
SORM	6.31	1.41E-10	132

The FORM analysis provides information on the influence of the stochastic variables to the variance of the limit state function. This is expressed by the so-called importance factor α^2 . A chart showing the different contributions is shown in Figure 5-2. The greatest influence to the reliability index is given by the log(C2) value considered in the SN-curve and the model uncertainty Δ in the Miner's rule.

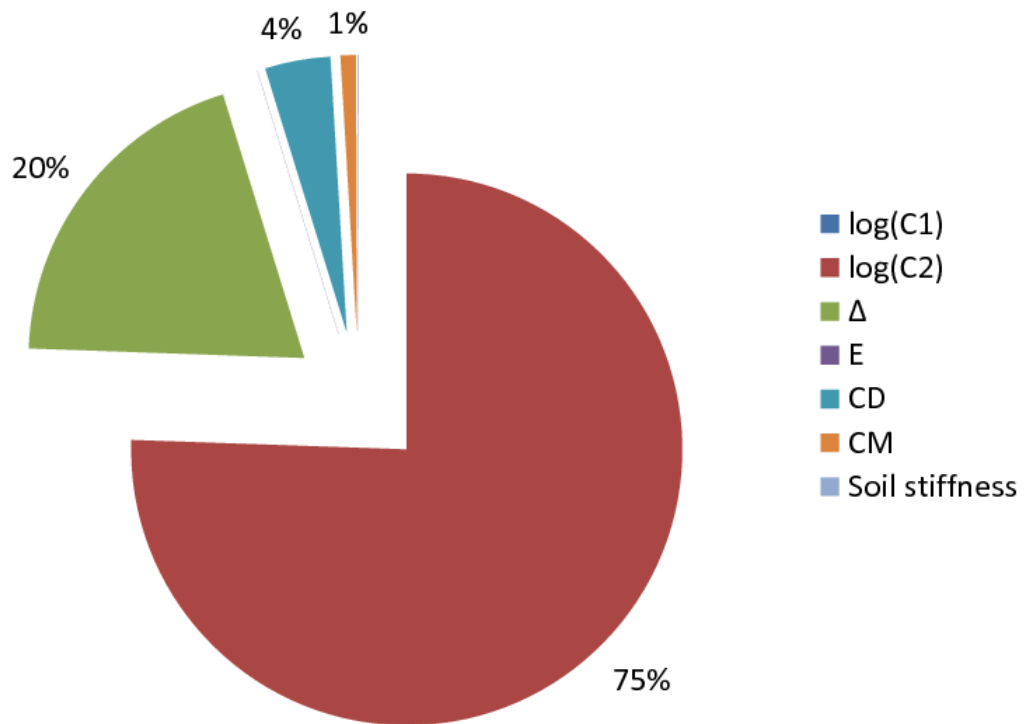


Figure 5-2 Influence of the stochastic variables to the variance of the limit state function.

Given the strong influence shown by two parameters, two additional reliability campaigns are performed to verify the sensitivity of the reliability index factor to a reduced parameter set. The use of a reduced number of stochastic variables leads to a reduced computational time. The subset of stochastic variables is:

- Campaign 2a: log(C1), log(C2), Δ, C_M, Soil stiffness.
- Campaign 2b: log(C1), log(C2), Δ, C_D, C_M.

The results for these campaigns are reported in Table 5-5. The difference between the first and second campaign in reliability index β and failure probability p_F values is very small.

Table 5-5 Results for the second reliability analysis campaigns.

Campaign	Analysis	β [-]	p_F [-]	LSF calls [-]
2a	FORM	6.32	1.28E-10	183
	SORM	6.28	1.68E-10	144
2b	FORM	6.37	9.39E-11	175
	SORM	6.37	9.37E-11	64

5.3.3 Conclusions

The present work shows how the integration of full load calculations with TURBU and probabilistic design method (FORM and SORM) is accomplished by linking a limit state function to the fatigue load at mudline.

The coupled tool was adopted to perform the reliability analysis of a 4 MW reference wind turbine. The results show how the main contributors to the variance of the limit state function are the uncertainty on the Miner's model Δ and the $\log(C2)$ parameter in the SN-curve. The analysis moreover shows that the reliability index for the full parameter set and for parameter sub-sets is higher than recommended by DNV-GL. There is therefore room for design optimization.

6. Ultimate buckling limit state

In this chapter, the limit state function for ultimate loads will be developed. For this ultimate limit state function, the characteristic 50-year load is needed. This characteristic load is determined based on extreme value statistics. First the determination of the characteristic load will be discussed followed by the selection of the limit state function.

6.1 Statistical extrapolation of wind turbine responses

6.1.1 Introduction

During its lifetime a wind turbine is subjected to a variety of wind conditions and wave conditions. Both wind and waves are of stochastic nature and should be accounted for during the wind turbine design. For the wind turbine responses driven by the environmental conditions like the blade and tower loads and displacements, an extreme response analysis is required. In the case of ultimate wind turbine responses, extreme value statistics should be applied to the wind turbine responses. A general introduction in extreme value statistics can be found in [12, 5, 7]. More information about the extreme value analysis for wind energy application can be found in [6, 19, 20].

In load case DLC 1.1 of the third edition of the IEC61400-1 standard [13], the ultimate responses during power production are estimated using extreme value theory. Aim of this statistical extrapolation is to determine the extreme load with a return period of 50 year. This means that the mean period between two 50-year responses is 50 year. In order to calculate the 50-year extreme response L_{50} , the long-term extreme response distribution needs to be estimated. This long-term extreme response distribution is found by integrating the long-term environmental distribution with the short-term extreme response distribution. The long-term response distribution F_{long} is the weighted average (convolution) of the conditional short-term probability distribution per mean wind speed of the response L is given by:

$$F_{long} = \int_v F_{short}(L|u) f_u(u) du$$

In [13], the long-term environmental distribution is a Weibull distribution of the 10-minute mean wind speed $f_u(u)$. The wind speed series is divided in a number of wind speed bins and, for every bin, simulations are performed with a state of the art aeroelastic tools. All the important features

of the wind turbine are captured with this approach. The design loads are calculated using a turbulence wind model to account for the stochastic nature of the wind. For every wind bin, a number of simulations are performed using different turbulent wind fields having the same mean wind speed and turbulence. Because of the different turbulent wind fields, every simulation will result in a different maximum load. Using these maxima, a short-term extreme response distribution $F_{short}(L|u)$ conditional on the wind speed is estimated for every wind speed bin. By using wind speed bins, the integration is changed in a summation

$$F_{long}(L) = \sum_i F_{short}(L|u_i) f_u(u_i) \Delta u_i$$

$$Q_{long}(L) = 1 - F_{long}(L) = \sum_i (1 - F_{short}(L|u_i)) f_u(u_i) \Delta u_i$$

Instead of the long-term extreme response distribution F_{long} , the probability of exceedance distribution Q_{long} is used to determine the 50-year response L_{50} . In the reliability analysis, the wind and wave loads and responses are simulated over 1-hour periods. This means that the probability of exceedance level associated with a 50-year return period should be based on the number of 1-hour periods during 50 year

$$Q_{long}(L_{50}) = \frac{1}{50 \times 365 \times 24} = 2.3 \times 10^{-6}$$

Important parameters in the statistical extrapolation process are:

- The number of time series (simulations) needed per wind speed bin;
- Selection of maximum or minimum responses from time series for every wind bin;
- Estimation of conditional short-term probability distributions;
- Estimation of 50-year response.

For the reliability analysis, the selected approach is described next.

6.1.2 Number of time series and data selection

The first question to be answered in the case of a statistical extrapolation analysis of wind turbine responses is the number of simulations needed to estimate a 50-year response. The number of time series depends on the number of maxima selected from a time series. The extreme value analysis is performed based on the selected maxima in the time series. Three data selection methods are available:

4. Global maxima;
5. Block maxima;
6. Peak Over Threshold (POT) maxima.

The main difference between the Global maxima method, the Block maxima method and the Peak Over Threshold method is the amount of data used from every 1-hour time series.

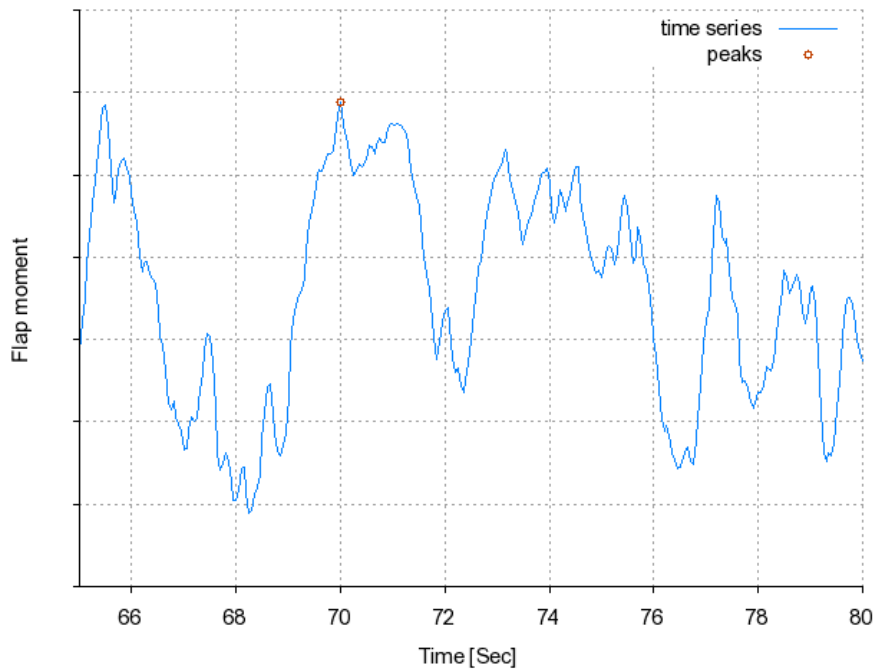


Figure 6-1 Example of a global maximum.

The Global maximum selection uses only one peak for the entire time series, see Figure 6-1. The Block maximum method and the Peak Over Threshold (POT) method use more peaks (maxima) for the time series. In the Block maximum method, the time series is divided by cutting the time series in a number of blocks and taking the maximum in each block. See Figure 6-2. The number of blocks should not be too large, because in the statistical extrapolation analysis it is assumed that the maxima are independent. For operating wind turbines this means that a sufficient number of blade revolutions should be considered. In the reliability analysis, the number of 1-hour time series per wind bin is 10 and the block size is 100s (i.e. 36 blocks per 1-hour, 360 blocks per bin).

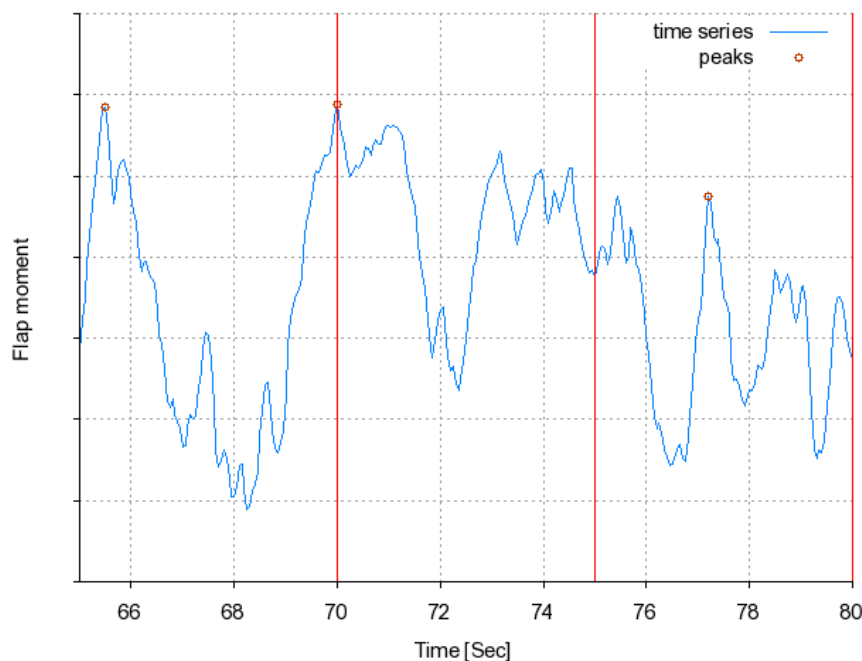


Figure 6-2 Example of selection of block maxima.

6.1.3 Short-term probability distributions

Since TURBU is a linear aeroelastic code, the response time series are also linear. This means that the time series is normal distributed, the amplitudes of the time series are Rayleigh distributed and the maxima of the time series are Gumbel distributed. For this reason the Gumbel distribution is selected as the short-term extreme response distribution F_{short} .

$$F_{Gumbel}(L|u) = \exp(-\exp(-\frac{L-\xi}{\alpha}))$$

The Gumbel distribution is defined for a response L with α as the scale parameter and ξ as the location parameter.

Aim of the statistical extrapolation of the wind turbine responses is to determine the 50-year response of the wind turbine. For this 50-year response to be estimated, a long-term distribution of the extreme response is needed.

For the Block maxima method and the POT method, the short-term distribution has to be transformed to the 1-hour equivalent short-term distribution $F_{1-hour}(L|u)$. When only the global maximum of each time series is used the short-term distribution is

$$F_{1-hour}(L|u) = F_{short}(L|u)$$

The short-term distribution for the Block maxima refers to a distribution for a maxima in a block. For a distribution of the maxima in a period of 1-hour, the short-term distribution of block maxima is transformed with the number of blocks n_b in a time period T as in equation :

$$F_{1-hour}(L|u) = F_{short}(L|u)^{n_b}$$

To determine the 50-year response, the long-term exceedance probability distribution Q_{long} is considered. The 50-year response is estimated numerically using the Regula Falsi (False Position) method. In the Regula Falsi method we are looking for the response L corresponding with the function $g(L) = Q_{long}(L) - 2.3 \cdot 10^{-6} = 0.0$.

6.2 Selection of Ultimate Limit State function

For the definition of the limit state for the ultimate loads, the approach from Uys [28] is followed. Two limit state function are defined: one for the yield stress f_y and one based on the critical buckling stress σ_{cr} .

For yield:

$$g = f_y - \sigma_{nom}$$

For buckling:

$$g = \sigma_{cr} - \sigma_{nom}$$

The nominal normal stress σ_{nom} is defined as:

$$\sigma_{nom} = \frac{N_j}{A_j} + \frac{M_j D_j}{I_j 2}$$

where N_j is the axial force, M_j the bending moment, A_j the cross sectional area, I_j the inertia and D_j the average diameter of the j^{th} section. The axial force and the bending moment are the 50-year loads based on statistical extrapolation.

The critical buckling stress of the j^{th} segment is given by DNV-RP-C202 recommended practice [10].

$$\sigma_{crj} = \frac{f_y}{\sqrt{1 + \lambda_j^4}}$$

$$\lambda_j^2 = \frac{f_y}{\sigma_{aj} + \sigma_{bj}} \left(\frac{\sigma_{aj}}{\sigma_{Eaj}} + \frac{\sigma_{bj}}{\sigma_{Ebj}} \right)$$

$$\sigma_{Eaj} = (1.5 - 50 \beta) C_{aj} \frac{\pi^2 E}{12(1 - \nu^2)} \left(\frac{t_j}{L_{ej}} \right)^2$$

$$\sigma_{Ebj} = (1.5 - 50 \beta) C_{bj} \frac{\pi^2 E}{12(1 - \nu^2)} \left(\frac{t_j}{L_{ej}} \right)^2$$

$$C_{aj} = \sqrt{1 + (\rho_a \zeta)^2} \text{ and } C_{bj} = \sqrt{1 + (\rho_b \zeta)^2}$$

$$\rho_a = 0.5 \left(1 + \frac{R_{avj}}{150 t_j} \right)^{0.5} \text{ and } \rho_b = 0.5 \left(1 + \frac{R_{avj}}{300 t_j} \right)^{-0.5}$$

$$\zeta = 0.702Z$$

$$Z = \frac{L_{ej}^2}{R_{avj} t} \sqrt{1 - \nu^2}$$

β is 0.02 [28].

In the buckling analysis only the monopile section above the mudline is considered with a length $L_e = 30\text{m}$.

6.3 Results

In the report the results of the structural reliability assessment of buckling are presented. Aa fully integrated load analysis is performed within the structural reliability analysis. The selected stochastic variables in the analysis are given in Table 6-1. Note that a model uncertainty X_{dyn} is included taking into account the uncertainty in the dynamics.

Table 6-1 Selected stochastic variables in buckling limit state analysis

Variable	Distribution	Mean	Standard deviation	References
Yield stress	Lognormal	240e6	12e6	
Young modulus	Lognormal	210e9	42e9	[26]
CM	Normal	2.00	0.10	[30]
CD	Normal	0.70	0.10	[30]
Soil stiffness	Lognormal	6.603e10	1.321e10	[30]
Xdyn	Lognormal	1	0.05	

The reliability index β and the probability of failure p_F are given in Table 6-2. Compared with the target reliability of 3.7 and the reliability index for fatigue of about 6, the ultimate state reliability is larger, being 14.0. It can be concluded that the ultimate limit state normal power production is not design driving for the monopile section at the seabed.

Table 6-2 The reliability index β and the probability of failure p_F for the buckling limit state.

Analysis	β [-]	p_F [-]
FORM	14.054	0

Table 6-3 gives the design point of the FORM analysis and the influence of the stochastic variables to the variance of the ultimate limit state function, the importance factor α^2 . The soil stiffness variable has the largest contribution to the variance of the limit state in this analysis, see also Figure 6-3. Keep in mind that a large change in soil stiffness affects the natural frequency of the wind turbine and, as a consequence, the dynamic loading. This effect is not accounted for during the analysis.

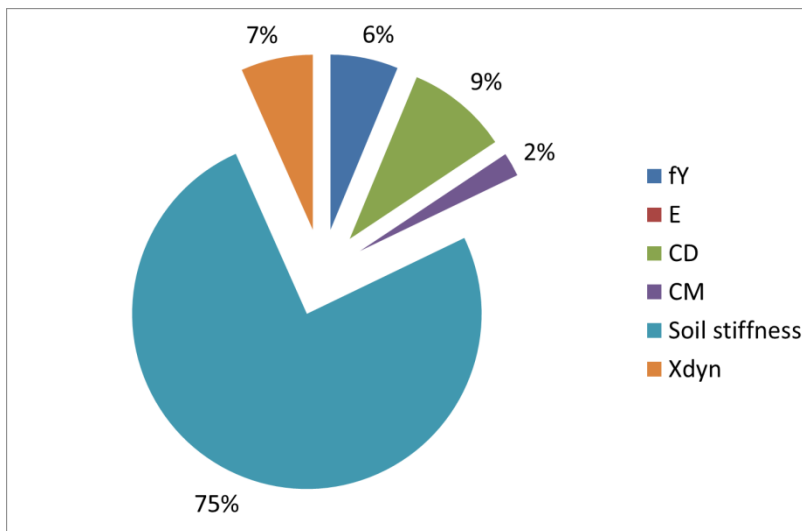


Figure 6-3 Influence of the stochastic variables to the variance of the ultimate limit state function

Table 6-3 Design point and Influence of the stochastic variables to the variance of the ultimate limit state function.

	Design point	Importance factor α^2
f _Y	1.47E+08	6%
E	2.10E+11	0%
C _D	0.93	9%
C _M	2.26	2%
Soil stiffness	1.01E+10	75%
X _{dyn}	1.64E+00	7%

7. Assessment of partial safety factors

In probabilistic design, the probability of failure and the reliability index β are determined. A monopile design is considered safe when the probability of failure is smaller than the target probability of failure. In practice, however, the industry designs a monopile according to the standard using partial safety factors. When a probabilistic design approach is applied, the first question from industry is how the reliability index relates to the partial safety factor prescribed by the standard. The translation of a probability of failure to the partial safety factors in the standard is not straightforward. Therefore the approach of determining partial safety factors is discussed first. See also the D4REL reliability framework report [2].

The DNV-GL and IEC standards are based on the Load and Resistance Factor Design (LFRD) method. The uncertainties and variability in the load strength S and material resistance R are introduced by partial safety factors. For a safe design, the characteristic load strength S_k multiplied by the load safety factor γ_f is smaller than the characteristic material resistance R_k divided by the material safety factor γ_m .

$$\gamma_f S_k \leq \frac{R_k}{\gamma_m}$$

In code calibration, it is common that the characteristic value of the load strength S_k is selected as the 98% percentile, while the characteristic value of the material resistance R_k is often the 5% percentile. For model uncertainties, like X_{dyn} in the buckling limit state, the mean is taken as characteristic value. The relation between the design point calculated in the probabilistic analysis and the partial safety factors is;

$$S_d = \gamma_f S_k$$

$$R_d = \frac{R_k}{\gamma_m}$$

In the design standard, the partial safety factors are prescribed for a given design load case with only one value for the strength load and one for the material resistance. Table 7-1 shows the partial safety factors from the standard for the limit states considered in the project. In the D4REL project, for both the fatigue and ultimate limit state only the normal production design load cases are considered. In each of the limit states, more than two stochastic variables are used. A

distinction is made between material resistance stochastic variables and load strength stochastic variables. For each of the stochastic variables in the probabilistic analysis, the associated partial safety factor is calculated. No attempt was made to derive single load and material partial safety factors for limit state. In case of a limit state with two stochastic variables R and S , the estimation of the partial safety factors is straightforward. In that case R determines the material safety factor and S the load safety factor of the limit state.

Table 7-1 Partial safety factors for limit states as defined by the standards.

Limit state	γ_f	γ_m
Fatigue limit state	1	1.25
Ultimate limit state	1.35	1.1

For the fatigue limit state, Table 7-2 shows the stochastic variable used together with the design point value, the characteristic value and the corresponding calculated partial safety factor (PSF). It can be seen that the partial safety factor for the stochastic variables $\log(C_1)$ and the soil stiffness are below 1. However the contribution to the total variance of the limit state function g is almost zero. The largest contribution to the variance is from $\log(C_2)$ with a partial safety factor slightly above one.

Table 7-2 Partial safety factors of the stochastic variables used in the fatigue limit state.

var	Design point	char value	PSF	Importance factor α^2	α
Strength					
Δ	0.418	1	2.39	0.197	0.444
$\log(C_1)$	12.164	11.764	0.97	0.000	0
$\log(C_2)$	14.722	15.606	1.06	0.756	0.869
E	2.10E+11	2.00E+11	0.95	0.000	0
Soil stiffnes	5.96E+10	4.67E+10	0.78	0.001	0.022
Loads					
C_D	0.814	0.7	1.16	0.038	0.196
C_M	2.127	2	1.06	0.009	0.094

Table 7-3 Partial safety factors of the partial safety factors used in the buckling limit state.

var	Design point	char value	PSF	α^2	alpha
Strength					
f_y	1.47E+08	2.21E+08	1.51	0.063	0.250
E	2.10E+11	2.00E+11	0.95	0	0
C_{soil}	1.01E+10	4.67E+10	4.61	0.755	0.869
Loads					
C_D	0.93	0.7	1.33	0.094	0.307
C_M	2.26	2	1.13	0.022	0.148
X_{dyn}	1.64E+00	1	1.64	0.067	0.258

In case of the buckling limit state, Table 7-3, the largest contribution to the limit state variance comes from the soil stiffness variable. The associated partial safety factor, 4.6, is well above 1.1. It should be noted that this is based on the assumption that the soil stiffness is part of the material resistance. As is the case for the fatigue limit state, again some stochastic variables have a partial safety factor value below the standard. For this reason, on the assessment of the partial safety factors alone, it is difficult to conclude that the design is conservative.

Although the probabilistic analysis shows conservatism in the design when comparing the reliability indices, this cannot directly be translated into large safety factors. As Winterstein stated[33], absolute p_F values should be interpreted carefully, as they depend on the precise choice of probability model adopted. The probabilistic analysis is perhaps best used in a relative sense: while one may question the absolute β values obtained, the relative β values across different designs can reasonably be used to suggest their relative safety levels.

8. Uncertainty of soil properties

During the D4REL project, the industry partners had the opportunity to propose research activities on probabilistic design. Based on the results of the fatigue analysis, it was proposed to model the uncertainties in the soil properties to investigate the relative contribution of the soil properties to the total variance of the limit state function g .

For this investigation, a limit state function is selected with a direct relation between the pile penetration and the soil-pile stiffness. For a given pile penetration and loading, the soil-pile stiffness is calculated based on p-y curves as defined in the standard [11].

Segeren and Diepenveen [24] state that the pile deflections in the soil under ULS need to fulfil the requirements:

- Maximum deflection at mud line $\leq Dmp/100m$
- Maximum deflection at pile toe $\leq 0.02m$
- Maximum influence of the penetration depth on the natural frequency 0.1%.

Where Dmp is the diameter of the monopile.

Carswell [32] gives maximum deflection u and rotation ϕ at the mudline as limit states

$$g = 0.7 - \phi$$

$$g = 0.2 - u$$

Here the deflection at the mudline of 0.2m is selected as limit state during the probabilistic analysis. The deflection is directly calculated by the open source software tool LatpilePY [1].

For the probabilistic analysis, information about the statistics of the soil layers is needed. For Sheringham Shoal, information is available in literature [16] and used in this study. The selected soil consists of three layers: the Boulders Bank formation (BDK), the Egmond Ground formation (EG) and the Swarte Bank formation (SBK).

The depth range of the three layers is:

- BDK 0m – 10m
- EG 10m – 18m
- SBK 18m – 40m

Table 8-1 Distribution and statistical values of selected soil layers.

Soil	propertie	Distribution	mean	CoV %
BDK	Undrained shear strength S_u [kPa]	Lognormal	123	49
EG	Friction angle ϕ' [deg]	Lognormal	46	6
SBK	Undrained shear strength S_u [kPa]	Lognormal	376	53

For the clay layers BDK and SBK, the undrained shear strength S_u is the stochastic variable used as input for the p-y calculations. For the sand layer EG this is the friction angle ϕ' . The statistical values used in the analysis together with the probability distribution are given in Table 8-1. The ultimate wind and wave loads at the mudline are assumed to be deterministic.

In the probabilistic design analysis, the soil-pile interaction is calculated based on p-y curves, where the soil properties are input. The Egmond Ground formation consists of very dense sand with mean friction angle ϕ' of 46°. For the determination of the p-y curves in sand, the initial modulus of subgrade reaction k is needed. This modulus k depends on the friction angle. Unfortunately, the standard does not give values of k for friction angles larger than 40°. However in probabilistic design, the design point is searched in an optimization loop. Therefore it was decided to apply a polynomial fit to extrapolate k values for larger friction angles. Figure 8-1 shows the fit of the initial subgrade reaction modulus.

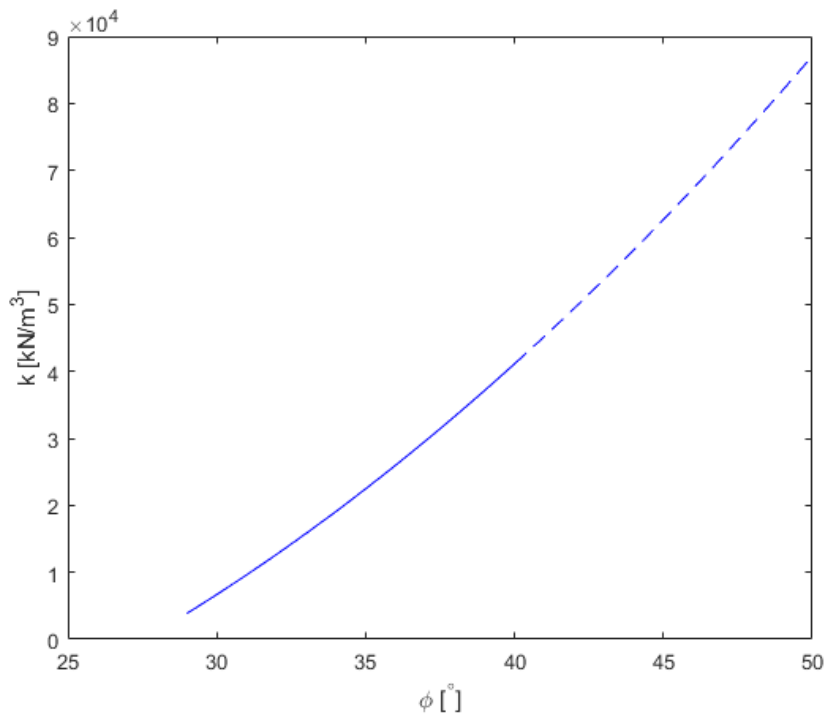


Figure 8-1 Polynomial fit of the initial modulus of subgrade reaction k with friction grade ϕ' .

The probabilistic analysis started with a pile penetration of 29m. The reliability index β for this pile penetration is 7.6. Table 8-2 shows that the deepest clay layer, Swarte Bank formation, has the largest influence on the variance of the limit state function. The analysis shows that assuming a target reliability index of 3.7, it might be possible to reduce the pile penetration. By step wise reduction of the pile penetration, see Figure 8-2, a reliability index of 3.9 is found for a pile penetration of 18m. Again the influence on the variance of the limit state function is largest for the clay layer. Now the Boulders Bank formation. See

Table 8-3. However, we have to consider the large coefficient of variance CoV of the stochastic variable S_u of about 50%.

Table 8-2 Design point at 29m pile penetration and influence of the stochastic soil variables on the variance of the limit state function.

	Design point	Importance factor α^2
BDK	3.97	11%
EG	38.97	5%
SBK	33.22	84%

Table 8-3 Design point at 18m pile penetration and influence of the stochastic soil variables on the variance of the limit state function.

	Design point	Importance factor α^2
BDK	22.30	90%
EG	42.75	10%
SBK	329.78	0%

This simple analysis shows the potential of reducing the pile penetration. However one should be aware that not only the pile deflection at the mudline is of importance, but also the constraints on the natural frequency of the support structure. In the current analysis the effect on the natural frequency is not taken into account. Besides that the p-y method to calculate the soil-pile interaction is simple compared to the finite element approach applied in the final design.

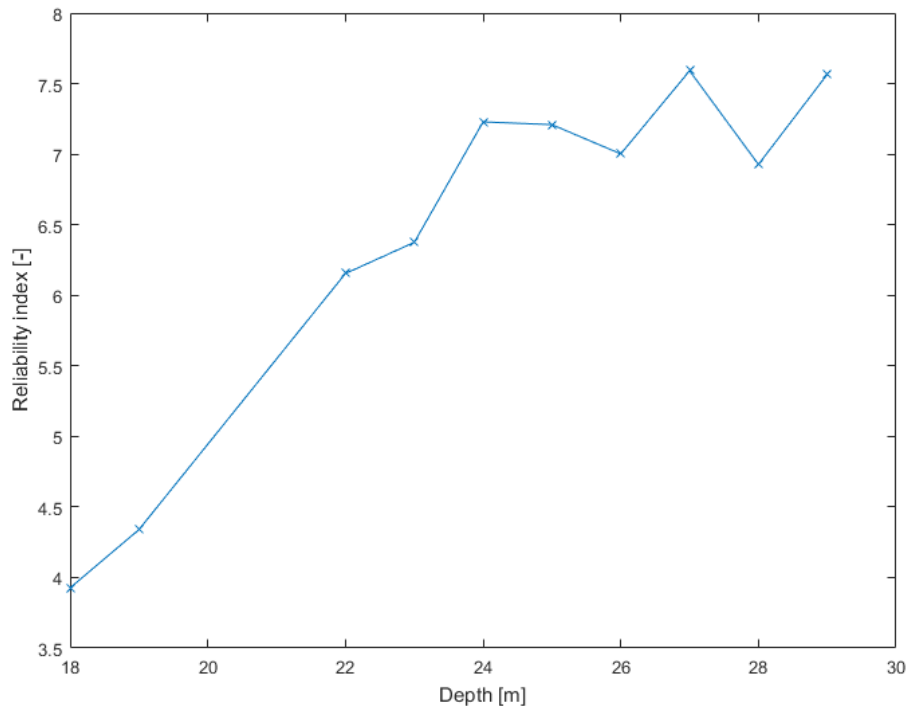


Figure 8-2 Pile penetration depth versus the reliability index β .

9. Conclusions

In work package 3 of the D4REL project a generic reliability analysis approach is developed for a monopile support structure. This means that the aeroelastic load calculations are incorporated in the reliability analysis. The analysis is performed by coupling the aeroelastic simulation tool TURBU with the open source reliability analysis tool FERUM. For the probabilistic analysis, a modern 4 MW offshore wind turbine is selected. Different reliability methods are available like the first order and second order reliability method, FORM and SORM, or methods based on Monte Carlo simulations. FORM is used since it calculated the contribution, importance factor, of the stochastic variables to the reliability.

In the probabilistic design approach, the limit state is considered. The limit state function g is the difference between the resistance R and the load L . For a safe design the limit function should be larger than zero. In structural reliability, the design point is determined where the limit state function is zero. Three limit state functions are considered:

1. A fatigue limit state;
2. An ultimate limit state on the yield stress;
3. An ultimate limit state on the global buckling stress.

The analysis shows how the main contributors to the variance of the fatigue limit state function are the uncertainty on the Miner's model Δ and the $\log(C2)$ parameter in the SN-curve. Moreover the reliability index for the full parameter set and for parameter sub-sets is higher than recommended by DNV-GL. There is therefore room for design optimization and cost reduction.

To investigate the sensitivity of the load analysis on the number of sea-states considered in the structural reliability analysis, three different sized data sets with sea states are considered.

1. A complete set of 20-year three-hours metocean hindcast data
2. 4D-histogram of binned mean wind speed u , significant wave height H_s , wave peak period T_p and wind wave misalignment θ ;
3. A lumped data set of 12 three-hour sea states.

For the fatigue limit state, the target reliability of DNV-GL is met by all data sets. However looking at the probability of failure, there is orders of difference. Based on the analysis, the lumped data set is the most conservative i.e. the highest probability of failure.

Ultimate load limit state analysis showed that the buckling limit state is dominating over the ultimate yield stress limit state. For the buckling limit state, a fully integrated load analysis is performed within the structural reliability analysis.

Compared to the target reliability of 3.7 and the reliability index for fatigue of 6, the ultimate state reliability is larger, being 14. It can be concluded that the ultimate limit state during normal power production is not design-driving for the monopile section at the seabed.

In probabilistic design the probability of failure and the reliability index β are determined. A monopile design is considered safe when the probability of failure is smaller than the target probability of failure. In practice, however, the industry designs a monopile according to the standard using partial safety factors. When a probabilistic design approach is applied, the first question from industry is how the reliability index relates to the partial safety factor prescribed by the standard. The translation of a probability of failure to the partial safety factors in the standard is not straightforward. Although the probabilistic analysis shows conservatism in the design when comparing the reliability indices, this is not directly translated to large safety factors. Not all the individual partial safety factors of the stochastic variables are higher than the values prescribed by the standard.

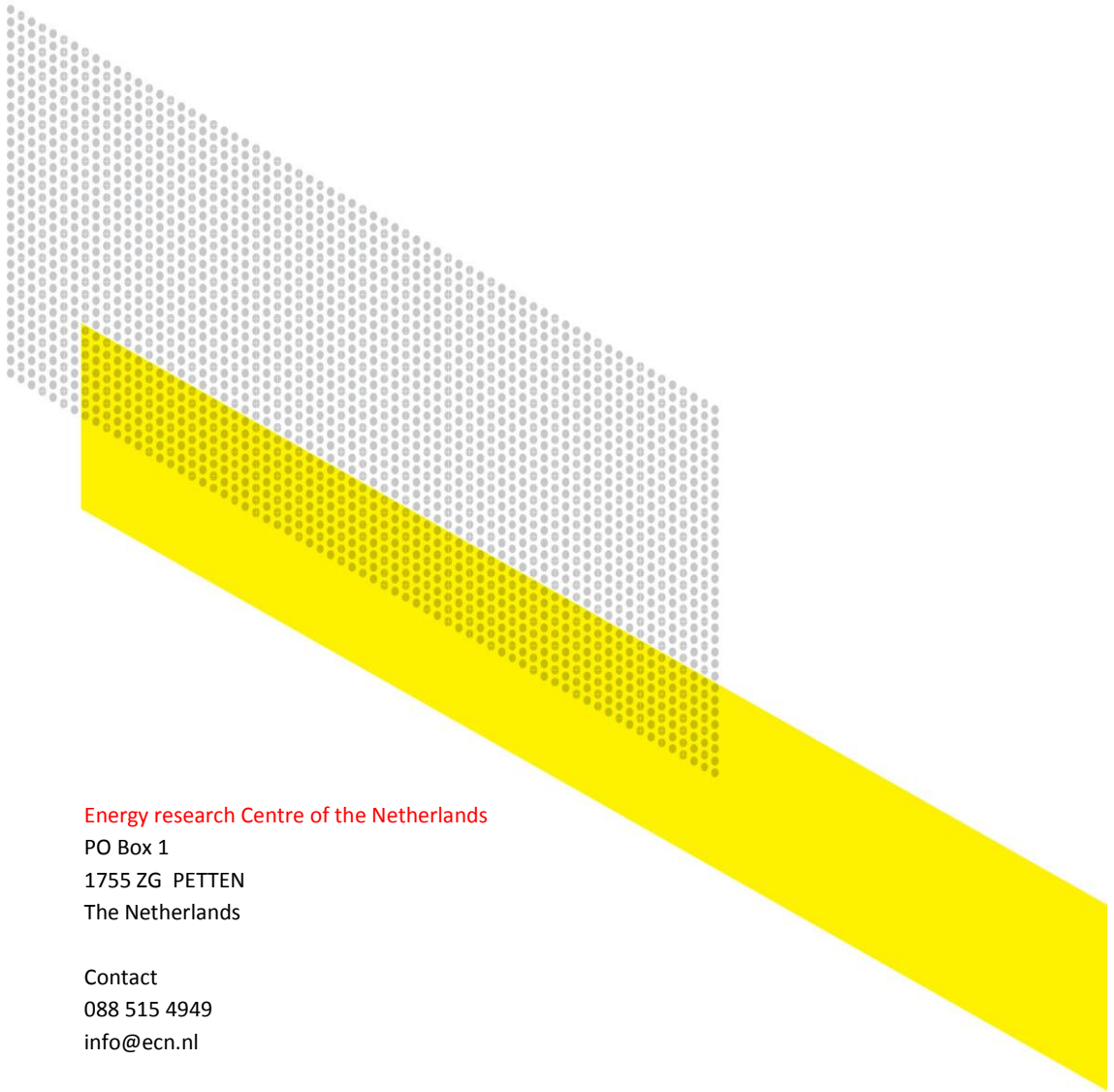
Finally during the D4REL project the industry partners had the opportunity to propose research activities on probabilistic design. Based on the results of the fatigue analysis it was proposed to model the uncertainties in the soil properties to investigate the relative contribution of the soil properties to the total variance of the limit state function g . The deflection at the mudline of 0.2m is selected as limit state during the probabilistic analysis. The deflection is directly calculated by the open source software tool LatpilePY. The probabilistic analysis shows that clay layer has the largest influence on the variance of the limit state function. However, we have to consider the large coefficient of variance CoV of the stochastic variable S_{cl} of about 50%.

In the D4REL project a structural reliability assessment of an existing design is performed. In future projects the developed probabilistic analysis method can be used in the design of support structures, where different concepts are compared.

Bibliography

- [1] Interactive design services pty ltd, "latpilepy v1.04."sep-2012.
- [2] M. Asgarpour and J.M. Peeringa. Frame work for reliability assessment of offshore wind support structures. Technical Report ECN-X-16-067, ECN, 2016.
- [3] K. Boorsma, T.S. Obdam, B.H. Bulder, O. Ceyhan, W. P. Engels, S.K. Kanev, F.J. Savenije, and T.W. Verbruggen. Smart rotor design - technology assessment. ECN report ECN-X-11-154, Petten, The Netherlands, December 2011.
- [4] J.-M. Bourinet, C. Mattrand, and V. Dubourg. A review of recent features and improvements added to FERUM software. In *Proceedings of the 10th International Conference on Structural Safety and Reliability (ICOSSAR'09)*, Osaka, Japan, 2009.
- [5] E. Castillo. *Extreme Value Theory in Engineering*. Academic Press Inc., San Diego, USA, 1988.
- [6] P. W. Cheng. *A reliability based design methodology for extreme responses of offshore wind turbines*. PhD thesis, Delft University of Technology, Delft, October 2002.
- [7] Stuart Coles. *An introduction to statistical modeling of extreme values*. Springer, 2001.
- [8] DNV. Environmental conditions and environmental loads. Recommended Practice DNV-RP-C205, Det Norske Veritas DNV, October 2010.
- [9] DNV. RPC-203 - Fatigue Design of Offshore Steel Structures, 2011.
- [10] DNV. Buckling strength of shells. RECOMMENDED PRACTICE DNV-RP-C202, DET NORSKE VERITAS AS, January 2013.
- [11] Det Norske Veritas AS DNV. Design of offshore wind turbine structures. Standard DNV-OS-J101, Det Norske Veritas AS (DNV), January 2013.
- [12] Emil Julius Gumbel. *Statistics of extremes*. Dover Publications, 2004.
- [13] IEC61400-1. Wind turbine generator systems - part 1: Safety requirements. Standard, International Electrotechnical Commission, August 2005.
- [14] JCSS (Joint committee of structural safety). Soil Properties (3.07). In *Probabilistic model code*. 2006.
- [15] Florian Ladage and Anja Brüning. Offshore wind farms gemini: Zeeenergie & buitengaats. updated metocean report. Technical report, DHIWASY GmbH, 2012.
- [16] Thi Minh Hue Le, Gudmund Reidar Eiksund, Pål Johannes Strøm, and Morten Saue. Geological and geotechnical characterisation for offshore wind turbine foundations: A case study of the sheringham shoal wind farm. *Engineering Geology*, 177(Supplement C):40 – 53, 2014.
- [17] C. Lindenburg. Phatas release "nov-2003" and "apr-2005" user's manual. program for horizontal axis wind turbine analysis and simulation. ECN report ECN-I-05-005, Energy research Centre of the Netherlands ECN, Petten, The Netherlands, May 2005.

- [18] Sergio Márquez-Domínguez and John Dalsgaard Sørensen. Fatigue Reliability and Calibration of Fatigue Design Factors for Offshore Wind Turbines. *Energies*, 5:234–241, 2002.
- [19] P. J. Moriarty, W. E. Holley, and S. P. Butterfield. Extrapolation of extreme and fatigue loads using probabilistic methods. Technical Report NREL/TP-500-34421, National Renewable Energy Laboratory NREL, Golden, Colorado, USA, September 2003.
- [20] J. M. Peeringa. Comparison of extreme load extrapolations using measured and calculated loads of a mw wind turbine. In *European Wind Energy Conference*, Marseille, France, March 2009. EWEA.
- [21] J.M. Peeringa. Wt-era users manual: Program for wind turbine - extreme response analysis. Technical Report ECN-E-10-055, ECN, 2010.
- [22] J.M. Peeringa and V. Bron. Wifi jip work package 2 - wave impacts on monopile. Technical Report ECN-X-14-047, ECN and Siemens Wind Power, 2014.
- [23] F. J. Savenije and J. M. Peeringa. Aero-elastic simulation of offshore wind turbines in the frequency domain, turbu@sea. Technical Report ECN-E-09-060, Energy research Centre of the Netherlands ECN, Petten, The Netherlands, 2009.
- [24] M.L.A. Segeren and N.F.B. Diepeveen. Influence of the rotor nacelle assembly mass on the design of monopile foundations. *Heron*, 59(1), 2014.
- [25] H. Snel and C. Lindenburg. Aeroelastic rotor system code for horizontal axis wind turbines: Phatas ii. In *European Community Wind Energy Conference*, Madrid, Spain, September 1990.
- [26] John D. Sørensen and Henrik S. Thoft, Probabilistic Design of Wind Turbines. *Energies*, 3(2):241–257, 2010.
- [27] John Dalsgaard Sørensen. Reliability analysis of wind turbines exposed to dynamic loads. In *Proceedings of the 9th International Conference on Structural Dynamics, EURODYN 2014*, number July, pages 39–46, Porto, Portugal, 2014.
- [28] P.E. Uys, J. Farkas, K. Jármai, and F. van Tonder. Optimisation of a steel tower for a wind turbine structure. *Engineering Structures*, 29(7):1337 – 1342, 2007.
- [29] T. G. van Engelen and H. Braam. Turbu offshore, computer program for frequency domain analysis of horizontal axis offshore wind turbines - implementation. Technical Report ECN-C-04-079, Energy research Centre of the Netherlands (ECN), Petten, The Netherlands, September 2004.
- [30] Dick Veldkamp. *Chances in Wind Energy; a probabilistic approach to wind turbine fatigue design*. PhD thesis, Delft University of Technology, 2006.
- [31] A.C.W.M. Vrouwenvelder and J.K. Vrijling. Probabilistisch ontwerpen. Technical Report Course notes b3, Technische universiteit Delft, 1987.
- [32] Carswell W., Arwade S.R., Myers A.T., and Hajjar J.F. Reliability analysis of monopile offshore wind turbine support structures. In *International Conference on Structural Safety and Reliability*, 2013.
- [33] Steven R. Winterstein. An introduction to structural reliability, form, and lfrd design. Technical Report PBE 2011-01, Probability based engineering, 2011.
- [34] Lisa Ziegler. Probabilistic estimation of fatigue loads on monopile-based offshore wind turbines. *M.Sc. Thesis - Delft University of Technology*, 2015.
- [35] Lisa Ziegler, Sven Voormeeren, Sebastian Schafirt, and Michael Muskulus. Design clustering of offshore wind turbines using probabilistic fatigue load estimation. *Renewable Energy*, 91:425–433, 2016.



Energy research Centre of the Netherlands

PO Box 1
1755 ZG PETTEN
The Netherlands

Contact
088 515 4949
info@ecn.nl

www.ecn.nl